

Experimental Investigation of Outlet-Manifold Effects in Jet-Impingement Boiling on Pin-Fin Surface using HFE-7000

Aqbal Ahmad¹, Shau-Wai Cheng¹ and Chi-Chuan Wang^{1*}

1 Affiliation of author: Department of Mechanical Engineering, National Yang Ming Chiao Tung University, Hsinchu, Taiwan 300

(Corresponding Author: Email: ccwang@nycu.edu.tw)

ABSTRACT

The study experimentally examines the influence of outlet-manifold on the thermal performance and thereby the energy efficiency of a two-phase jet-impingement cooling system using HFE-7000 as the working fluid, enabling more effective energy utilization in high-heat-flux applications. The test section features a fixed 3×16 jet array with a jet diameter of 1.5 mm and a jet-to-jet pitch of 2.5 mm. A comparative analysis is conducted between a symmetric double outlet manifold and a more compact single outlet (side-in/side-out) configuration, highlighting design choices that optimize energy transfer rates. Results demonstrate that the double-outlet design yields superior heat transfer performance across the operating range, exhibiting a consistently lower wall superheat at a given heat flux and a reduced thermal resistance, which collectively contribute to lower overall energy demands for cooling. A significant enhancement in critical heat flux (CHF) was observed, with the double-outlet manifold achieving 53 W/cm², compared to 29.1 W/cm² for the single-outlet design at a mass flux of 78 kg/m²·s, allowing for sustained high-power operation with minimized energy penalties. The lowest recorded thermal resistances were 0.036 °C/W for both manifold types, though the dual-outlet design sustained this performance over a broader range, promoting broader energy-efficient deployment. Furthermore, the study examines the impact of manifold design on temperature uniformity across the heated surface, revealing that the outlet configuration plays a critical role in mitigating temperature gradients and ensuring equitable energy distribution in thermal management systems.

Keywords: Heat transfer performance, jet impingement, CHF, thermal resistance.

NONMENCLATURE

A_D	Area of die/heater area (m ²)
I	Supplied current (A)
k	Thermal conductivity
Q	Heat load (W)
q''	Heat flux (W/cm ²)
R	Thermal resistance
T	Temperature (°C)

Abbreviations

ONB	Onset of Nucleate Boiling
HTC	Heat transfer coefficient
CHF	Critical heat flux

Symbols

w	Wall
in	Inlet

1. INTRODUCTION

The relentless miniaturization and increased integration of electronic components have precipitated a corresponding exponential rise in heat flux generation, with reported values exceeding 1000 W/cm² [1]. Effective thermal management is therefore critical to maintain device temperatures within a safe operational range, ensuring efficient performance and mitigating the risk of thermal failure [2]. Conventional single-phase cooling techniques, such as air-cooling and liquid cooling, are increasingly inadequate for dissipating such extreme heat fluxes, particularly within spatially constrained applications [3,4]. The two-phase cooling, presents a promising alternative by utilizing the latent heat of vaporization to extract substantial thermal energy with minimal temperature rise. Among prevalent two-phase cooling methods including immersion cooling, microchannel flow boiling, spray, and jet impingement each presents distinct limitations [5,6, 7]. A major limitation of immersion cooling is the extensive working-fluid demand of immersion cooling increases system cost

and complicates large-scale implementation. Microchannel flow boiling, while effective, can suffer from flow instabilities, significant pressure drops, and pronounced wall temperature gradients along the flow direction. The practical deployment of spray cooling systems is constrained by inherent design complexity, elevated maintenance requirements, and considerable spatial demand. In contrast, submerged jet array impingement cooling has emerged as a highly promising solution. It combines superior heat transfer performance with the distinct advantages of temperature uniformity and adaptability, making it exceptionally well-suited for managing both large heating areas and localized hot spots

Rau and Garimella [8] investigated confined single-jet impingement boiling on copper targets spanning a polished baseline, a microporous coating, square pin-fins, and a hybrid pin-fin surface over-coated with the porous layer. Using a 3.75 mm orifice at 0.45–1.80 L/min, they examined the effect of micro-/macro-scale topologies on thermal–hydraulic performance under confinement. The microporous film primarily enhanced nucleation-site density and liquid supply, raising the area-averaged nucleate-boiling heat-transfer coefficient (HTC) by up to 500% relative to the smooth surface. The pin-fin geometry mainly delayed dry out by enlarging the wetted area and promoting cross-flow redistribution. Combining both features yielded a synergistic hybrid response: critical heat flux (CHF) increased by 2.4 times without measurable increase in pressure drop, effectively decoupling thermal enhancement from hydraulic cost. The transition to vigorous boiling rendered momentum effects negligible, confirming that liquid replenishment and vapor evacuation were dominated by the porous-fin morphology instead of jet inertia.

Rau et al. [9] compared a 5 × 5 array of 0.75 mm jets matched in total orifice area to a 3.75 mm single jet impinging on four copper targets (polished flat, microporous coating, square pin-fins, and a hybrid pin-fin surface over-coated with the porous layer) to decouple momentum distribution from surface morphology. At identical volumetric flow rates, distributing the flow through the array increased single-phase heat-transfer coefficients (HTC) by 13–29% relative to the single jet, confirming the convective advantage of multi-jet impingement. In two-phase operation, performance was governed primarily by the target topology: the hybrid surface synergistically combined macro-scale vapor escape pathways with micro-scale wicking, extending the critical heat flux (CHF)

by 1.89–2.33 times versus the single jet on the same surface and larger than 4 times relative to the single jet on a smooth plate. The jet array on the hybrid target sustained 205.8 W/cm² (1.33 kW total) at only 10.9 kPa pressure drop.

Hui et al. [10] experimentally evaluated boiling heat-transfer performance when a 5 × 5 distributed array of 0.8 mm jets impinged on copper targets overlaid with open-cell metal-foam covers of systematically varied pore density (20–40 PPI), porosity (92–97%), thickness (3–5 mm) and wettability. Relative to the plain copper surface, an optimized 20 PPI, 94% porous, 3 mm-thick foam raised the critical heat flux (CHF) and peak heat-transfer coefficient (HTC) by 36.9% and 22.9%, respectively; the corresponding maxima reached 538 W/cm² and 57.9 kW/m² K at only 4 m/s jet velocity. Performance first improved and then declined as pore density increased, while lowering porosity or modestly thickening the foam (< 4 mm for 20 PPI) augmented capillary wicking and vapor-escape pathways and thicker or finer-pore foams-imposed conduction and flow resistance penalties. Wettability tailoring altered onset-of-nucleate-boiling (ONB) superheat by ±5 K, hydrophobic coatings accelerated incipience but slightly reduced peak HTC, whereas hydrophilic foams mitigated post-CHF deterioration. Bubble-visualization data confirmed that once vigorous nucleate boiling was established, HTC collapsed onto a single curve independent of jet momentum, indicating surface morphology governed liquid supply and vapor removal. Correlations developed for both single- and two-phase regimes predict HTC and CHF within ±10% across all geometries and operating conditions.

Ji et al. [11] designed a distributed, confined jet-array impingement boiling module with multiple local return (effusion) outlets and tested it using HFE-7100 on both smooth silicon and micro-pin-fin targets. Over mass flux 760–3040 kg/m² s at about 40 K inlet subcooling and atmospheric pressure, the distributed layout suppressed cross-flow, shortened vapor residence time, and delivered more uniform heat removal across the field than a conventional shared-outlet arrangement. Micro-pin-fin surfaces consistently reduced ONB superheat and raised HTC/CHF relative to smooth surfaces, while, in the fully developed boiling regime, local jet-position effects became negligible owing to the equalized cell-by-cell supply/exit. Ji et al. [12] Using high-speed imaging on a distributed jet, confined jet-array with HFE-7100, the study visualized near-wall two-phase morphology while varying jet mass flux and jet-to-surface height. The key observations were that distributed (local-return) outlets

suppress lateral plume coalescence and large-scale vapor clouds, thereby reducing cross-flow interference, shortening vapor residence, and stabilizing boiling compared with shared-outlet arrangements. Increasing mass flux and optimizing jet height promoted frequent, smaller bubble departure and more uniform cell-by-cell evacuation, consistent with improved heat-transfer uniformity reported in their companion experiments.

Prior studies [8–12] largely pursue heat-transfer enhancement in jet-impingement boiling by distributing momentum through multi-jet arrays and by tailoring target-surface morphology often combining both to intensify liquid replenishment and accelerate vapor removal via distributed flow paths. While the influence of outlet-manifold topology on boiling heat transfer performance remains comparatively underexplored, leaving limited evidence for its impact on heat-transfer coefficients, critical heat flux, pressure drop, and temperature non-uniformity. To address this gap, the present work provides a controlled experimental assessment of outlet-manifold design in a confined jet-impingement heat sink, quantifying its effects on area-averaged heat transfer and on heat sink base temperature non-uniformity relevant to electronics cooling.

2. EXPERIMENTAL METHODS

2.1 Fluid flow loop

The experimental facility shown in the **Figure 1** is a closed-loop flow-boiling setup built to quantify the thermal and hydraulic performance of a hybrid jet-impingement microchannel heat sink using HFE-7000. The loop integrates a fluid reservoir, a variable-speed gear pump (Micro-pump GB-P25-P-V-S-A), an electrically heated test section, a plate-type condenser, and a unified instrumentation suite. The reservoir provides inventory control and pressure buffering, accommodating volumetric changes associated with

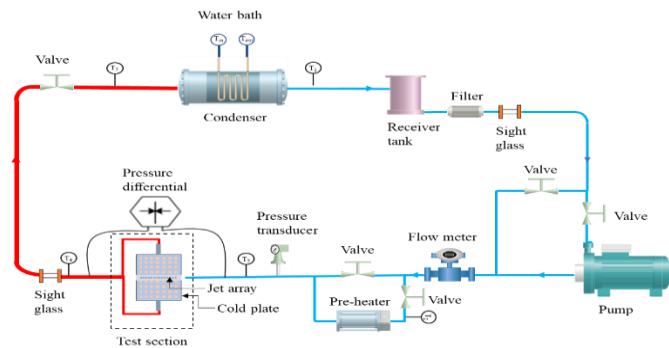


Figure 1 Schematic diagram of experimental setup

phase change and ensuring a continuous supply of liquid coolant. Flow conditions are imposed by the gear pump and verified in real time with a Coriolis flowmeter (CoriMate II-CR004), which yields density- and pressure-independent mass-flow measurements suitable for two-phase operation. The test section comprises a lid surface capped by a jet-impingement cover and mounted on a thermal test vehicle (TTV) that supplies controllable electrical power. Multiple thermocouples embedded along the flow direction and within the lid base map the temperature field with high spatial resolution, while inline pressure transducers (FP201A-D 31-L20A) and a differential transmitter (EJA110M) record absolute pressure and pressure drop. Downstream, the two-phase working fluid is condensed in a plate-type heat exchanger using a secondary water loop, returning subcooled liquid to the reservoir and closing the circuit. All sensors and power channels are integrated into a centralized data-acquisition system (MX100, Yokogawa) that records synchronized, high-fidelity thermal, hydraulic, and electrical signals. This architecture provides a controlled, repeatable environment for rigorous characterization of boiling curves, heat-transfer coefficients, and pressure-drop behavior across a broad operating envelope.

2.2 Test section assembly

Figure 2 details a purpose-built jet-impingement flow-boiling module assembled from six precision-machined parts that are stacked, sealed, and pre-loaded by through-bolts. Working upward from the base, the first element is the thermal-test vehicle (TTV), a calibrated resistive heater that replicates the heat flux of an electronic die. A thermal grease of high thermal conductivity ($k = 14 \text{ W/m K}$) is placed between the lid and TTV. The lid, fabricated from oxygen-free copper for minimal spreading resistance, incorporates blind holes

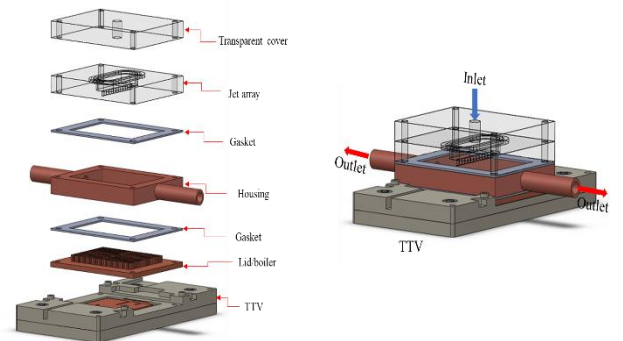


Figure 2. Test section assembly

for five T-type micro-thermocouples that measure the local wall temperature distribution.

A rubber gasket provides the primary static seal

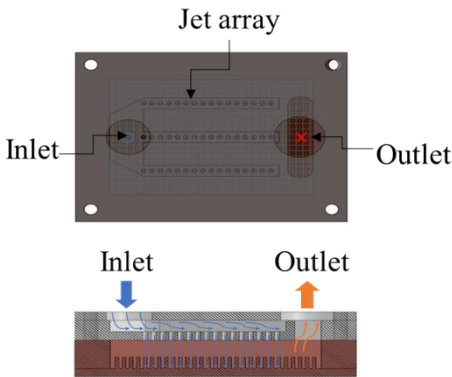
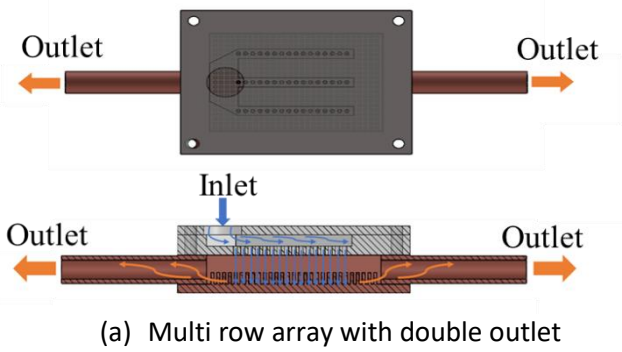


Figure 3 Configurations of inlet/outlet manifolds and jet arrays

between the lid and the overlying copper housing. The housing forms an annular plenum that receives two-phase working fluid from the boiling surface and directs it toward a pair of diametrically opposed outlet. A second gasket isolates the housing from the jet-array plate, which is machined from optically clear polycarbonate to permit visualization. This plate contains a square array of precision-drilled orifices (1.5 mm diameter, jet pitch 2.5 mm) that accelerate the incoming liquid into discrete, high-momentum micro-jets.

The uppermost transparent cover also polycarbonate forms the inlet manifold. A single centrally located inlet port admits sub-cooled liquid, which is distributed by the jet-array plate and impinges perpendicularly on the heated lid, initiating vigorous boiling. A concentric O-ring compressed between the jet plate and the cover constitutes the final pressure boundary, preventing leakage of the dielectric working fluid.

During operation, liquid delivered through the top manifold is fragmented into jets (inlet temperature = 27°C), impinges on the boiling surface, and rapidly vaporizes. The resulting two-phase mixture is swept laterally into the housing plenum and expelled through the double outlets, thereby minimizing pressure drop while preserving high local heat-transfer coefficients. The modular design affords excellent optical access for high-speed imaging, straightforward replacement of jet plates with alternative geometries, and reliable, repeatable sealing for extended experimental operations.

2.3 Inlet and outlet flow arrangements design

Outlet and manifold topology exert first-order control over two-phase transport in compact heat sinks. In confined jet-array modules, well-designed outlets lower two-phase back-pressure, shorten vapor residence time, suppress density-wave oscillations, and thereby lift both heat-transfer coefficients and the critical heat flux (CHF). In this work, we systematically vary the inlet/outlet manifolds and the jet arrangement to optimize jet-impingement boiling over a pin-fin surface. The two configurations are summarized in **Figure 3**. Figure 3(a) has a single inlet and bilateral outlets but distributes multiple jet rows across the center region producing a more uniform liquid supply. The paired outlets promptly remove working fluid from both sides, mitigating cross-flow sweeping of downstream jets and reducing lateral pressure gradients. In Figure 3(b), the working fluid enters from a lateral plenum on one short side, traverses above the jet plate, and exits through a lateral plenum on the opposite side. This classical through-flow is simple to plumb and can lower manifold losses, but the superposed cross-flow tends to deflect downstream jets and thicken the two-phase boundary layer toward the outlet, promoting temperature non-uniformity at high heat flux.

2.4 Data analysis

The total power supplied to system is given by;

$$Q = V \times I \quad (1)$$

where V and I are the DC voltage and current supplied to TTV.

The heat flux is calculated as follows:

$$q'' = \frac{Q}{A_{Die}} \quad (2)$$

where A_{Die} is the area of die or heater area.

Heat transfer coefficient is calculated as:

$$HTC = \frac{q''}{(T_w - T_{in})} \quad (3)$$

The thermal resistance is given by:

$$R_{th} = \frac{(T_w - T_{in})}{Q} \quad (4)$$

2.5 Uncertainty analysis

The uncertainty associated with derived parameter is calculated as given in [13, 14] as follows;

$$u_p = \sqrt{\sum_{i=1}^n \left(\frac{\partial p}{\partial a_i} u_i \right)^2} \quad (5)$$

Where u_p is uncertainty associated with the derived parameter p which is functions of a_i and u_i is uncertainty associated with parameter a_i .

The uncertainty associated with heat flux is calculated using Eq. (5) and given as:

$$\frac{u_{q''}}{q''} = \left(\left(\frac{u_I}{I} \right)^2 + \left(\frac{u_V}{V} \right)^2 + \left(\frac{u_{A_c}}{A_c} \right)^2 \right)^{1/2} \quad (6)$$

The uncertainty associated with Thermal resistance is calculated using Eq. (5) and given as:

$$\frac{u_{R_{th}}}{R_{th}} = \left(\left(\frac{u_{q''}}{q''} \right)^2 + \left(\frac{u_{\Delta T}}{\Delta T} \right)^2 \right)^{1/2} \quad (7)$$

The maximum uncertainty for heat flux, degree of wall superheat and thermal resistance are 3.18%, 1.07 % and 3.36%, respectively.

3. RESULTS

The present work aims investigate the effect of outlet-manifold topology on two-phase jet-impingement boiling in HFE-7000 for a fixed jet array (1.5 mm diameter, 2.5 mm pitch and jets normal to the lid). Two confined modules were compared, a symmetric dual-outlet design that evacuates the working fluid radially toward opposite sides, and a more compact single-outlet design that collects all working fluid to one exit. The study compares a symmetric dual-outlet manifold with a compact single-outlet variant thermal performance. Across the operating range, the outlet architecture produced clear, repeatable differences in thermal performance. At a given heat flux, the double outlet manifold sustained lower wall superheat and higher area-averaged HTC. The advantage widened beyond ONB and became most pronounced near CHF, where vapor removal limits performance. The side-in/side-out manifold showed stronger two-phase cross-flow interference, evidenced by a steeper rise in temperature with heat flux and an earlier approach to dry out. These

trends are consistent with physical mechanisms, the double outlet manifold shortens vapor evacuation paths, reduces residence time in the impingement zone, and preserves liquid replenishment at the stagnation core, whereas the side-in/side-out manifold concentrates spent two-phase flow toward one side, elevating local void fraction.

3. 1 Effect of Outlet Manifolds Design on Jet Impingement Boiling Performance

The Fig. 4 shows the boiling curves of the pin-fin surface for two different outlet manifold designs at the mass flux of 78 kg/m² s. In the low heat flux region, the heat transfer is dominated by forced convection, and the flux increases linearly with wall to inlet superheat. When the heat flux increased beyond the ONB, the slope of the boiling curve increases sharply and slope of curve start decreasing as heat approaches to critical heat flux due to partial vapor coverage of heated surface. The graph shows that the double outlets manifold sustains high heat flux before reaching to critical heat flux as compared to side-in/side outlet. This is due to fact that the symmetric double-outlet manifold evacuates vapor more effectively and sustains liquid replenishment at the impingement core, delaying partial dry out whereas the side-in/side-out layout concentrates spent two-phase flow toward a single exit, elevating local void fraction and cross-flow interference. The critical heat flux for double outlet manifold is 53 W/cm² compared to 29.1W/cm² for side in/side outlet at mass flux of 78 kg/m²s. which is ~85% higher with double outlet manifold compared to side-in/side-outlet manifolds whereas at mass flux of 60 kg/m² s, the critical heat flux for double outlet manifolds are ~100% higher than side-in and side-outlet manifolds.

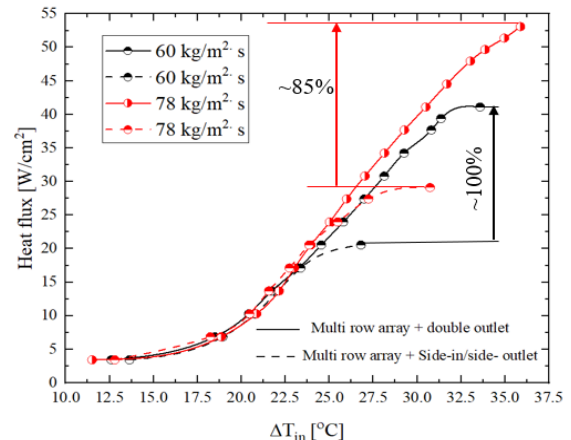


Figure 4 Boiling curve

Figure 5 compares the thermal resistance versus heat flux for the two outlet-manifold layouts at two different mass fluxes. Across the entire operating range, the double-outlet manifold maintains a consistently lower thermal resistance than the side-in/side-out design, indicating superior heat-transfer performance at a given heat load. The minimum thermal resistance achieved with the double-outlet module is 0.036 °C/W compared with 0.055 °C/W for the side-in/side-out configuration at mass flux of 78 kg/m²s . This advantage is attributed to

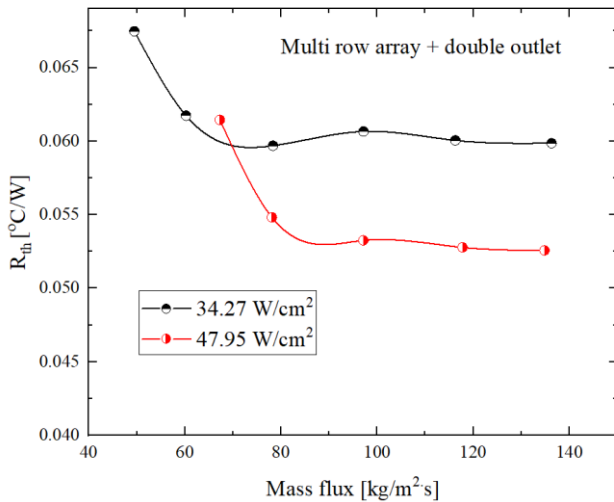


Figure 6 Thermal resistance variation with mass flux for Multi-row + double outlet manifolds more efficient vapor evacuation and reduced jet-to-jet interference in the double-outlet architecture, which preserve liquid replenishment at the stagnation core, suppress local vapor accumulation.

3. 2 Effect of mass and heat flux on Thermal Resistance in Pin-Fin Jet Impingement Boiling

Figure 6 reports the overall thermal resistance of the pin-fin surface with a multi-row jet array and a double-outlet manifold as a function of mass flux across several heat-flux set points. At low mass flux, the jets have insufficient momentum to efficiently rewet the surface, leading to a thicker liquid thermal boundary layer and sluggish bubble sweep-off, both effects elevate the wall temperature and yield a higher thermal resistance. Increasing the mass flux strengthens jet momentum, which thins the boundary layer, improves liquid replenishment within the fin field, and accelerates vapor removal.

Figure 6 shows that heat flux modulates the mass-flux sensitivity of the overall thermal resistance. At the lower heat flux (34.27 W/cm²), thermal resistance decreases only modestly with increasing mass flux and becomes relatively insensitive beyond 78 kg/m²s, consistent with a convection dominant boiling regime. At the higher heat flux (47.95 W/cm²), thermal resistance drops sharply as mass flux rises from 60.23 to 78 kg/m²s and then flatten at a lower level than the low-heat-flux case. This transition near 78 kg/m²s indicates that once vigorous boiling is established and vapor is efficiently cleared, liquid replenishment and vapor evacuation within the porous-fin field dominate the heat transfer, reducing thermal resistance and diminishing the influence of jet inertia at higher mass fluxes.

3. 3 Effect of Outlet Manifold Design on the temperature distribution

Figure 6 shows the streamwise temperature distribution on the pin-fin base at heat flux of 27.5 W/cm² for two different outlet manifold designs. With the double-outlet manifold, the profile is comparatively flat and the peak temperature remains modest around 56 °C. In contrast, the side-in/side-outlet manifold exhibits a pronounced asymmetry and a hot spot develops on the upstream side (78.5°C). The flatter, temperature profile with the double-outlet design indicates more uniform wetting and uniform nucleation across the surface, consistent with shorter vapor-evacuation paths. The single-outlet geometry concentrates spent flow toward one side, promoting plume coalescence and local void fraction buildup upstream, which elevates the wall temperature and degrades temperature uniformity.

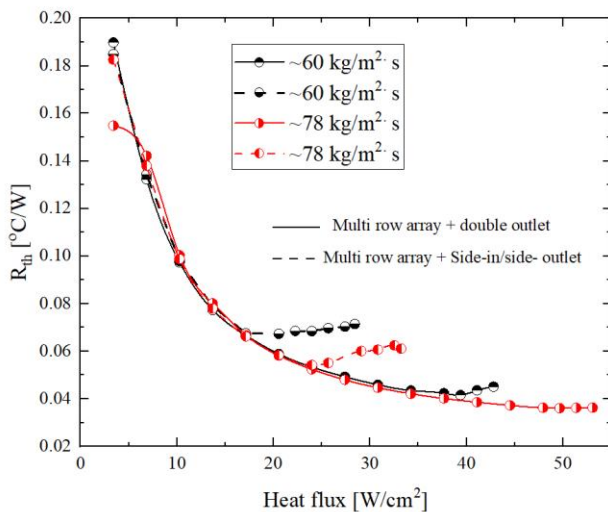


Figure 5 Thermal resistance variation with heat flux

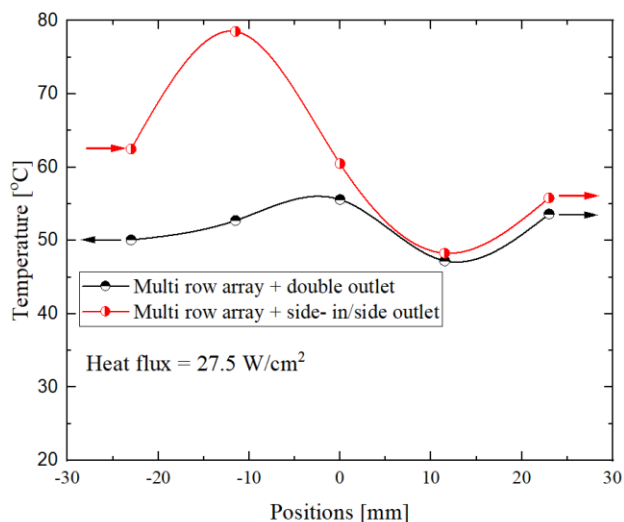


Figure 7. Temperature distribution

4. CONCLUSIONS

This study investigates the effect of outlet manifold designs on the heat transfer performance of confined jet impingement boiling on the pin-fin surface using HFE-7000 coolant. The two outlet design manifolds such as double outlet and side-in/side-outlet manifold is studied experimentally and their performance is compared in terms heat flux and thermal resistances. The results show that the double outlet manifold sustain high heat flux compared to side-in/side-outlet manifold and thermal resistance of double outlet manifold is lower than the side-in/side-outlet manifold. The critical heat flux for double outlet manifold is 53 W/cm^2 compared to 29.1 W/cm^2 for side-in/side-outlet at mass flux of $78 \text{ kg/m}^2 \cdot \text{s}$ and lowest resistance resistances for double outlet manifolds and side-in/side-outlet are $0.036 \text{ }^\circ\text{C/W}$ and $0.055 \text{ }^\circ\text{C/W}$ respectively. In addition to this, the study also investigates the temperature non-uniformity variation with outlet manifolds.

ACKNOWLEDGEMENT

The authors gratefully acknowledge the financial support from the National Science and Technology Council Taiwan under the contract NSTC 112-2221-E-A49-026.

REFERENCE

[1] Ebadian, M. A., and C. X. Lin. "A review of high-heat-flux heat removal technologies." (2011): 110801.

[2] Reliability prediction of electronic equipment. U.S. Department of Defense, MILHDBK-2178B, NTIS, Springfield, VA; 1974

[3] Huang, P. C., C. F. Yang, J. J. Hwang, and M. T. Chiu. "Enhancement of forced-convection cooling of multiple heated blocks in a channel using porous covers." *International journal of heat and mass transfer* 48, no. 3-4 (2005): 647-664.

[4] Gupta, Naveen Kumar, Arun Kumar Tiwari, and Subrata Kumar Ghosh. "Heat transfer mechanisms in heat pipes using nanofluids—A review." *Experimental Thermal and Fluid Science* 90 (2018): 84-100.

[5] Devahdhanush, V. S., and Issam Mudawar. "Review of critical heat flux (CHF) in jet impingement boiling." *International Journal of Heat and Mass Transfer* 169 (2021): 120893.

[6] G. Liang, I. Mudawar Review of pool boiling enhancement by surface modification. *Int. J. Heat Mass Transf.*, 128 (2019), pp. 892-933

[7] Yang, Xiao-Hu, Si-Cong Tan, and Jing Liu. "Thermal management of Li-ion battery with liquid metal." *Energy conversion and management* 117 (2016): 577-585.

[8] Rau, M.J., Garimella, S.V., "Confined Jet Impingement with Boiling on a Variety of Enhanced Surfaces," *Journal of Heat Transfer*, **136**(10) (2014) 101503.

[9] Rau, M.J., Garimella, S.V., Dede, E.M., Joshi, S.N., "Boiling Heat Transfer from an Array of Round Jets with Hybrid Surface Enhancements," *Journal of Heat Transfer*, **137**(7) (2015) 071501.

[10] Hui, Yao, Xuan Li, Rui Lei, Haitao Hu, and Yonghua Huang. "Boiling heat transfer characteristics of distributed jet array impingement on metal foam-covered surface." *International Journal of Heat and Mass Transfer* 233 (2024): 126038.

[11] Ji, X., Ma, X., Yang, X., Wei, J., Sundén, B., "Jet array impingement boiling in compact space for high heat flux cooling," *Applied Thermal Engineering*, **219** (2023) 119538.

[12] Ji, X., Yang, X., Ma, X., Tian, H., Wei, J., Sundén, B., "Two-phase flow characteristics and visualization of distributed confined array jet boiling," *Case Studies in Thermal Engineering*, **57** (2024) 104345.

[13] Holman, Jack Philip. *Experimental methods for engineers*. McGraw-Hill, 1971.

[14] Joshi, S.N., D.J. Lohan, and E.M. Dede, *Two-phase performance of a hybrid jet plus multipass microchannel heat sink*. *Journal of Thermal Science and Engineering Applications*, 2020. **12**(1): p. 011019